APPLIED SCIENCES AND ENGINEERING

Tissue-engineered vascular microphysiological platform to study immune modulation of xenograft rejection

Tae Hee Kim[1†], Ji-Jing Yan[2†], Joon Young Jang[2], Gwang-Min Lee[2,3], Sun-Kyung Lee[2,3], Beom Seok Kim[4], Justin J. Chung[1], Soo Hyun Kim[1], Youngmee Jung[1,5]*, Jaeseok Yang[2,6]*

Most of the vascular platforms currently being studied are lab-on-a-chip types that mimic capillary networks and are applied for vascular response analysis in vitro. However, these platforms have a limitation in clearly assessing the physiological phenomena of native blood vessels compared to in vivo evaluation. Here, we developed a simply fabricable tissue-engineered vascular microphysiological platform (TEVMP) with a three-dimensional (3D) vascular structure similar to an artery that can be applied for ex vivo and in vivo evaluation. Furthermore, we applied the TEVMP as ex vivo and in vivo screening systems to evaluate the effect of human CD200 (hCD200) overexpression in porcine endothelial cells (PECs) on vascular xenogeneic immune responses. These screening systems, in contrast to 2D in vitro and cellular xenotransplantation in vivo models, clearly demonstrated that hCD200 overexpression effectively suppressed vascular xenograft rejection. The TEVMP has a high potential as a platform to assess various vascular-related responses.

INTRODUCTION

Various tissue-engineered microphysiological platforms, which include organs-on-chips and organ replicas, have been studied for application in basic, pharmaceutical and medical sciences as simple and rapid investigation tools (*1*). In particular, since blood vessels are related to various fundamental physiological phenomena, including immune responses and human diseases, there is a great need to develop a vascular platform for research on them (*2*). Most of the currently developed vascular platforms are vessel-on-a-chip types and are applied as in vitro vascular disease models, vasculature in organ-on-chips, and drug screening platforms by mimicking capillary networks through angiogenesis or vasculogenesis (*3*–*6*). Yasotharan *et al.* (*7*) proposed an artery-on a-chip that can evaluate the calcium dynamic response to abluminal stimulation. In most cases, these vascular platforms fabricated a randomly formed capillary-like vascular structure through the self-assembly of endothelial cells (ECs) in hydrogels or were manufactured by coating ECs on the channel wall of a chip composed of synthetic polymers (e.g., polydimethylsiloxane), which is mechanically and physiologically different from the native vessel. These are useful tools for simply evaluating the physiological phenomena of blood vessels in vitro, but they have some limitations in clearly analyzing the physiological phenomena of native blood vessels, such as in vivo assessment. To compensate for these limitations, we fabricated a tissue-engineered vascular microphysiological platform (TEVMP), which can be applied not only in vitro but also in vivo, with a three-dimensional (3D) vascular structure similar to an artery.

[1]Center for Biomaterials, Biomedical Research Institute, Korea Institute of Science and Technology (KIST), Seoul, Republic of Korea. [2]Biomedical Research Institute, Seoul National University Hospital, Seoul, Republic of Korea. [3]Department of Medicine, Graduate School, Seoul National University College of Medicine, Seoul, Republic of Korea. [4]Division of Nephrology, Department of Internal Medicine, Yonsei University College of Medicine, Seoul, Republic of Korea. [5]School of Electrical and Electronic Engineering, YU-KIST Institute, Yonsei University, Seoul, Republic of Korea. [6]Transplantation Center, Seoul National University hospital, Seoul, Republic of Korea.
*Corresponding author. Email: jcyjs@snu.ac.kr (J.Y.); winnie97@kist.re.kr (Y.J.)
†These authors contributed equally to this work.

Tissue-engineered vascular graft (TEVG) studies have been conducted in various ways for a long time (*8*). Many studies have fabricated TEVGs using biodegradable synthetic polymers (e.g., polyglycolic acid, polylactic acid, and polycaprolactone) or allogeneic and xenogeneic decellularized tissues as materials for constituting TEVG scaffolds. These scaffolds were additionally treated with various natural components, such as collagen and fibrin, to induce vascular cell adhesion and differentiation. Furthermore, in these scaffolds, mural cells (e.g., vascular smooth muscle cells, fibroblasts, and pericytes) and ECs were cocultured to mimic mature blood vessels (*9*). However, the intended application of most TEVG studies has been to provide vascular replacements for clinical vascular implantation. The corresponding fabrication processes are complex and time consuming. For these reasons, it is inefficient to apply these TEVG fabrication processes as vascular screening platforms. The TEVMP developed in this study was designed to be fabricated quickly using a simple process to apply a TEVG as a vascular screening tool. TEVMP was fabricated through a simple plastic compression process using collagen and fibrin hydrogels, which are the main components of the extracellular matrix (ECM) that compose blood vessels. The greatest shortcoming of hydrogel scaffolds is their weak mechanical properties. The plastic compression process allows a notable and rapid increase in the scaffold strength, as it removes water from the hydrogels and increases their density (*10*). Unlike previous studies that introduced dense scaffolds fabricated with either collagen or fibrin hydrogels by the same principle and method (*11*, *12*), collagen-fibrin hybrid gels were used in this study. Scaffolds fabricated using only collagen or fibrin hydrogels are difficult to use as vascular structures because of their low elasticity or stiffness, even when plastic compression is introduced (*13*). Therefore, hybrid gels containing collagen, which increases stiffness, and fibrin, which increases elasticity, were used, and a plastic compression process was introduced to improve the mechanical properties of the TEVMP.

Organ transplantation is the treatment of choice for patients with end-stage organ failure; however, organ shortage is an important

hurdle. Xenotransplantation could be a potential alternative to mitigate aggravating discrepancies between organ needs and organ supply. Because immune rejection in xenografts is much stronger than that in human allografts, xenograft rejection remains the main hurdle to successful clinical application, and we need to develop better immune modulation strategies to suppress xenograft rejection. One of the strategies to suppress xenograft rejection is the genetic modification of donor pigs that could reduce systemic immunosuppression to avoid heavy immunosuppression-related adverse events. The successful introduction of α1,3-galactosyltransferase gene-knockout pigs (*14*) and human complement regulatory protein-transgenic pigs such as hCD46-transgenic pigs (*15*) could avoid catastrophic hyperacute rejection and prolong xenograft survival (*16*); however, acute vascular rejection remains a challenge to be overcome (*14*, *17*, *18*). CD200 is a well-known inhibitory molecule that suppresses macrophages and antigen-presenting cells as well as T cells, which are involved in acute vascular xenograft rejection (*19*–*21*). Previous studies have reported that CD200 suppresses rat-to-mouse cellular xenograft rejection and cellular allograft rejection (*22*, *23*). Furthermore, our previous study demonstrated that overexpression of human CD200 (hCD200) in porcine ECs (PECs) showed the best suppressive effects against acute cellular xenograft rejection compared to overexpression of human CD47 (hCD47) through in vitro and cellular xenotransplantation using a humanized mouse model (*24*). However, these studies showed beneficial effects of CD200 for suppressing only cellular rejection in cellular xenotransplantation models. They could not demonstrate the impact of hCD200 overexpression on vascular rejection, which is a stronger rejection than cellular rejection and a key obstacle to successful organ xenotransplantation (*25*).

There remain some challenges with introducing hCD200 into transgenic pigs to test the beneficial effects of hCD200 overexpression on vascular xenograft rejection. Since the generation of transgenic pigs requires complicated processes, a long time, and high cost, before generation, more convenient screening tests targeting vascular xenograft rejection should be performed in a human microenvironment using native tissue-like 3D platforms. The TEVMP could be a potential alternative, mimicking the human vascular system for testing the effects of hCD200. In this study, we applied the TEVMP as an ex vivo and in vivo screening tool as a bioartificial blood vessel mimicking the native blood vessels of hCD200-transgenic pigs to evaluate the effect of hCD200 on vascular xenograft rejection in the human circulatory system–like microenvironment.

The overall study scheme from the generation of TEVMPs for ex vivo and in vivo functional studies is shown in Fig. 1. PECs that overexpress hCD200 or hCD47 were injected into the lumen of TEVMPs to endothelialize TEVMPs with PECs (pTEVMPs) as an alternative to the blood vessels of transgenic pigs. After that, the pTEVMP was applied to an ex vivo screening system, where human whole blood was perfused into the pTEVMP through the microfluidic system, and an in vivo screening system, where the pTEVMP xenograft was transplanted into humanized mice, to investigate the immune regulatory roles of hCD200 and hCD47 against vascular xenograft rejection. We proved the promising roles of this pTEVMP not only as an ex vivo vascular platform but also as an in vivo vascular platform in vascular xenotransplantation to humanized mice and found that overexpression of hCD200 in PECs successfully suppressed the xenogeneic immune response, including vascular xenograft rejection.

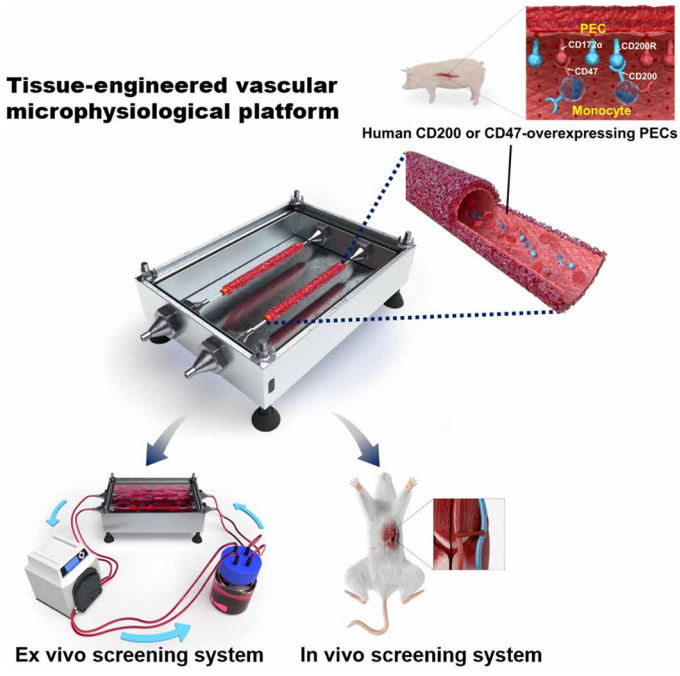

Fig. 1. Overall schematic illustration of the study. The overall study scheme from the generation of pTEVMPs to ex vivo and in vivo functional studies is illustrated. TEVMPs were fabricated via plastic compression and endothelialized with hCD200- or hCD47-overexpressing PECs. Using these pTEVMPs, the roles of hCD200 and hCD47 in PECs were evaluated in an ex vivo circulation system and in vivo vascular xenotransplantation to humanized mice as screening systems.

RESULTS

Generation of pTEVMP

Physiologically and mechanically stable TEVMPs are produced through the following series of processes (Fig. 2A): A 1-ml syringe with a rod inserted in the center was loaded with a collagen-fibrin hybrid solution to form a structure that mimics the vascular lumen. After gelation of the hybrid solution, a high-density compression TEVMP was fabricated through a modified plastic compression technique. The fabricated TEVMPs were mounted in custom-made vascular perfusion chambers, and suspended PECs were injected into the lumen of the TEVMPs for endothelialization. Thereafter, pTEVMPs were connected to the microfluidic system, and the culture media of PECs were perfused into the lumen of pTEVMPs under physiological blood flow conditions for 1 day. Figure 2B shows the forms of the TEVMP before and after plastic compression. The external diameter of the TEVMP decreased from 5.11 ± 0.10 mm to 1.53 ± 0.02 mm after plastic compression, while the inner diameters were 819 and 815.99 ± 54.64 μm before and after compression, respectively, showing similar values.

The mechanical strength and stability of the pTEVMP

To evaluate the mechanical properties of the TEVMP, burst pressure and tensile testing were performed in three groups (Fig. 2C): the TEVMP fabricated by collagen with plastic compression (Col-PC group), the TEVMP fabricated by collagen-fibrin hybrid gels without plastic compression (Hybrid group), and the TEVMP fabricated by collagen-fibrin hybrid gels with plastic compression (Hybrid-PC group). The Hybrid-PC group showed a high burst pressure value that was approximately two times higher than that of

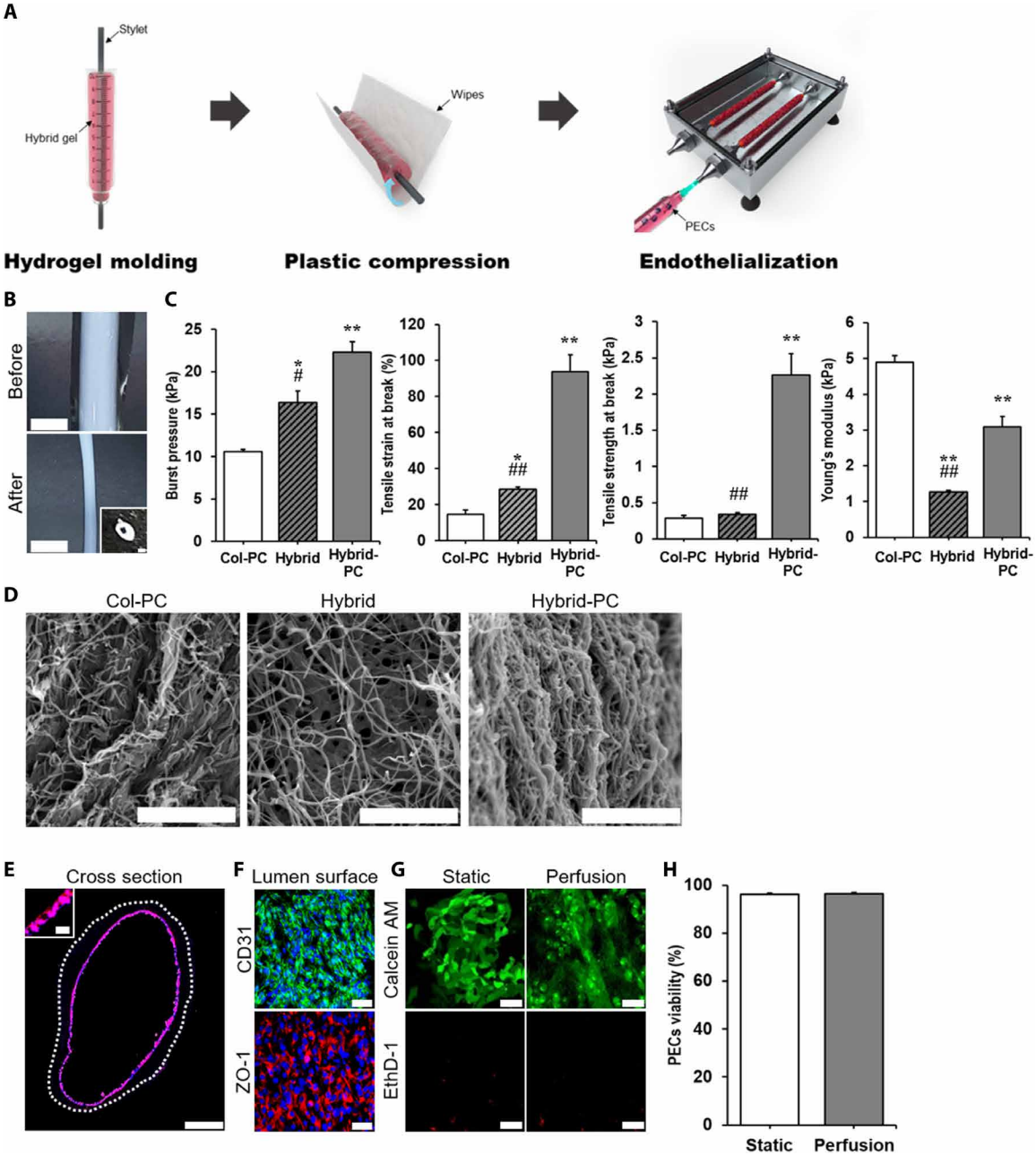

Fig. 2. Generation and characterization of the pTEVMP. (**A**) Process of the TEVMP fabrication and endothelialization with genetically engineered PECs. The TEVMP was fabricated by a modified plastic compression process of collagen-fibrin hybrid gels. hCD200-, hCD47-, or hCD200/CD47-overexpressing PECs as well as control PECs with mock vector were seeded into the lumen of TEVMPs to make pTEVMPs. (**B**) TEVMPs before (top) and after (bottom) compression. The inset shows a cross view of the TEVMP. Scale bars, 500 μm. (**C**) Mechanical properties of the TEVMP, including the burst pressure, tensile strain, and Young's modulus. Data are expressed as the means ± SEM. *$P < 0.05$ and **$P < 0.01$ compared to the collagen group, and #$P < 0.05$ and ##$P < 0.01$ compared to the Hybrid-PC group. (**D**) Cross-sectional SEM image of collagen with plastic compression, hybrid gels without plastic compression, and hybrid gels with plastic compression. Scale bars, 5 μm. (**E**) Cross-sectional rhodamine phalloidin staining of pTEVMPs after perfusing PECs for 1 day. Rhodmine phalloidin is red and DAPI is blue. The white dotted contour indicates the pTEVMP outline. Scale bar, 200 μm. The inset shows a magnification of the pTEVMP cross-sectional wall. Scale bar, 20 μm (**F**) Representative immunofluorescence images of intracellular junction proteins, including CD31 (green) and ZO-1 (red), in the lumen of pTEVMPs after perfusion for 1 day. Scale bars, 50 μm. (**G**) A LIVE/DEAD assay for PECs in the lumen of pTEVMPs was performed using calcein AM (green) and EthD-1 (red) staining. Scale bars, 50 μm. (**H**) Quantification of the cell viability in the pTEVMP lumen in the static and perfusion groups.

the Col-PC group and approximately 1.4 times higher than that of the Hybrid group. The tensile testing of the Hybrid-PC group TEVMP was determined by using a universal testing machine, and three values (strain at break, strength at break, and Young's modulus) were obtained and compared to those of the Col-PC and Hybrid groups. The tensile strain and strength at break for the Hybrid-PC group were significantly higher than those of the Hybrid group and Col-PC group ($P < 0.01$). For the Hybrid group, the tensile strain

was higher than that of the Col-PC group ($P < 0.05$), but the tensile strength was not significantly different from that of the Col-PC group ($P = 0.32$). The examination of Young's modulus revealed that the highest value was in the Col-PC group, followed by the Hybrid-PC group and Hybrid group (4.89 ± 0.18 kPa in the Col-PC group, 1.26 ± 0.058 kPa in the Hybrid group, and 3.09 ± 0.30 kPa in the Hybrid-PC group). Together, these mechanical property results indicate that the TEVMP of the Hybrid-PC group has the highest elasticity among the three groups and higher stiffness than that of the Hybrid group TEVMP. Figure 2D shows the cross-sectional surface morphology of each group of hydrogels analyzed by scanning electron microscopy. The Col-PC group fabricated by collagen formed bundles of fibers of uniform thickness, but the Hybrid and Hybrid-PC groups fabricated by hybrid gels were formed by mixing thin and thick fibers. In the Col-PC and Hybrid-PC groups subjected to plastic compression, the fibers were arranged in a layered structure, whereas in the Hybrid group, the fibers showed a loose net structure.

The distributions of PECs, intercellular junctions, and viability were investigated to confirm the effect of the shear stress generated during perfusion with physiological blood flow conditions on the PECs endothelialized in TEVMPs. In the cross-sectional image, F-actin stained with phalloidin was expressed throughout the lumen of pTEVMPs perfused for 1 day, indicating that PECs were not detached by shear stress and were evenly distributed throughout the vessel wall of TEVMPs (Fig. 2E). Figure 2F shows that intercellular junction markers, such as cluster of differentiation 31 (CD31) and zonula occludens-1 (ZO-1), were expressed uniformly and continuously at the cell-cell edges of the pTEVMP lumen surface. Moreover, in perfused pTEVMPs, the viability of PECs was 96.28 ± 0.57%, which was similar to that of PECs cultured under static conditions (96.11 ± 0.57%) (Fig. 2, G and F). These results indicate that PECs formed a stabilized endothelium through the high cell adhesion ratio and formation of intercellular junctions in the lumen of the TEVMP, and thus, the pTEVMP could be used as an artificial vascular platform in the physiological blood flow environment.

Impact of hCD200 in PECs on in vitro immune responses

PECs were transduced with lentiviruses containing the mock vector, hCD47, hCD200, or both hCD200 and hCD47 to overexpress hCD200 or hCD47. In the coculture of PECs and human peripheral blood mononuclear cells (hPBMCs) in the presence of human plasma (Fig. 3A), both hCD200 and hCD47 in PECs suppressed the phagocytic activity of hPBMCs against PECs (Fig. 3B). Next, hCD200 in PECs suppressed apoptosis of PECs (annexin V^+pCD31^+) and increased the viability of PECs [7-aminoactinomycin D $(7\text{-AAD})^-pCD31^+$] against the cytotoxic activity of hPBMCs (Fig. 3C). hCD200 in PECs also suppressed the levels of tumor necrosis factor–α (TNF-α), interleukin-1β (IL-1β), and IL-6 (Fig. 3D). These results demonstrate that the overexpression of hCD200 in PECs successfully suppressed the xenogeneic immune response by human immune cells and xenoreactive antibodies.

Impact of hCD200 on ex vivo immune responses toward the pTEVMP

To assess the impact of the overexpression of hCD200 or hCD47 in PECs on xenogeneic immune responses, we established an ex vivo pTEVMP circulation system as follows: TEVMPs were endothelialized with normal PECs (control group), hCD47-overexpressing PECs (CD47 group), hCD200-overexpressing PECs (CD200 group), and hCD200/hCD47-overexpressing PECs (double group) and perfused with PBMCs or human whole blood as physiological blood flow.

When hPBMCs and human plasma were perfused through pTEVMPs, hCD200 in PECs suppressed xenogeneic immune responses in the pTEMVP circulation system (fig. S1). The survival of PECs was estimated by flow cytometry analysis of porcine CD31 (pCD31; fig. S1A). The number of surviving PECs was higher in the CD200 and double groups than in the control group, while the CD47 group showed no significant difference from the control group. To confirm the interactions between PECs and human inflammatory cells, we evaluated immunofluorescence staining results for human CD68, a marker of macrophages, and human CD3, a marker of T cells (fig. S1B). In the CD200 group, both human $CD68^+$ and $CD3^+$ densities were approximately 5 and 17 times lower than those of the control group, respectively (fig. S1B). In particular, the human $CD3^+$ cell density of the CD200 group was remarkably lower than that of the CD47 group and the double group ($P < 0.01$). In addition, analysis of the perfusate obtained by the perfusion of hPBMCs and human plasma using the pTEVMP circulation system was performed. Similar to the in vitro evaluation, the levels of TNF-α, IL-1β, and IL-6 were very low in the CD200 group compared to the control group (fig. S1C). The levels of complement components 3a (C3a) and 5a (C5a) in the perfusates were significantly reduced in the CD200 group (Cont. versus CD200: $P < 0.01$; CD47 versus CD200: $P < 0.05$) (fig. S1D). In the case of the CD47 group, C5a was remarkably decreased compared to the control group ($P < 0.01$), but C3a did not show a significant difference from the control group.

Next, human whole blood was perfused in each group of pTEVMPs to estimate vascular xenograft rejection ex vivo (Figs. 4 and 5). Apoptosis of PECs was determined using immunofluorescence staining of caspase 3 (Fig. 4A). The caspase 3^+ cell density to the $pCD31^+$ cells was the lowest in the CD200 group, followed by the double group, CD47 group, and, lastly, the control group (fig. S2A). In parallel, the number of 7-AAD^-pCD31^+ cells analyzed by flow cytometry was higher in the CD200 group than in the other three groups (Fig. 4B). The double group had a higher survival of PECs than the control group, and the CD47 group did not differ significantly from the control group. These data indicate that hCD200 in PECs suppressed PEC apoptosis and improved PEC survival to a greater extent than hCD47 and the double overexpression of hCD200/CD47. Figure 4C and fig. S2B indicate infiltration of human inflammatory cells and complement deposition in each group of pTEVMPs. $CD68^+$ macrophage and $CD3^+$ T cell densities showed significantly lower expression in the CD200 group than in the CD47 and double groups as well as the control group ($P < 0.01$). These results demonstrated that hCD200 in PECs suppressed the infiltration of $CD68^+$ macrophages and $CD3^+$ T cells into the pTEVMP tissues to a greater extent than hCD47. Moreover, hCD200 in PECs showed better suppressive effects on the deposition of antibodies and complement in pTEVMP tissues than hCD47. Immunoglobulin G (IgG) is the most common type of antibody found in blood circulation, which is a major component of humoral immunity and activates all the classical pathways of the complement system (*26*). C4d is a marker of antibody-mediated rejection as a by-product of complement activation via the classic pathway by antibody-antigen complexes (*27*). The CD200 group significantly decreased the human IgG^+ and $C4d^+$ area density in the pTEVMP better than the control and CD47

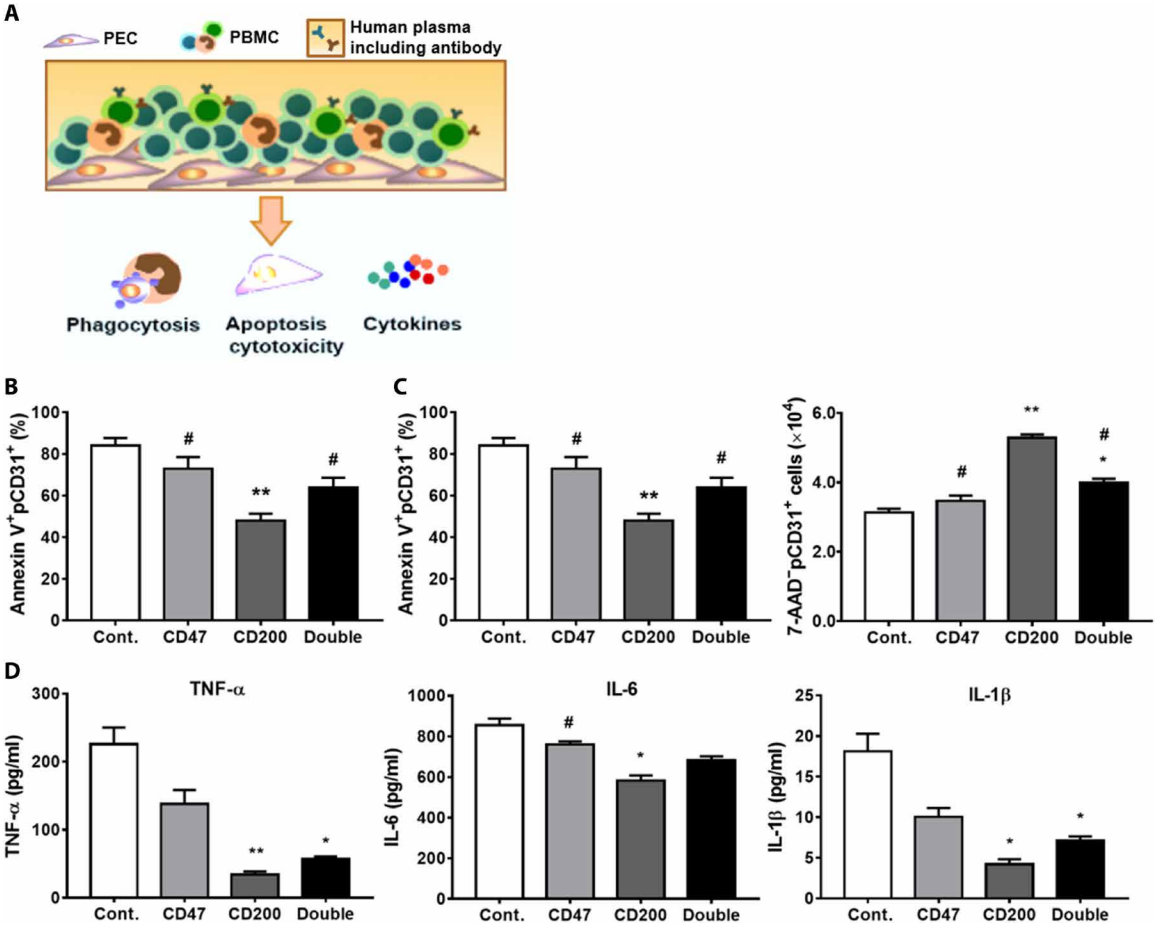

Fig. 3. hCD200 suppressed in vitro xenogeneic immune responses by hPBMC in the presence of human plasma. (**A**) In vitro experimental scheme. After PECs were incubated with hPBMC with 20% human plasma, phagocytosis, cytotoxicity, and cytokine production were assessed. (**B**) Suppressive activity of hCD200 and hCD47 against the phagocytic activity of hPBMC toward PECs. (**C**) Suppressive activity of hCD200 and hCD47 against apoptosis of PECs (annexin V^+CD31^+). Impact of hCD200 and hCD47 on live PECs ($7\text{-}AAD^-CD31^+$). (**D**) Suppressive activity of hCD200 and hCD47 against secretion of proinflammatory cytokines (TNF-α, IL-1β, and IL-6) from hPBMCs in response to PECs. $n = 4$ to 5 per group. Data are expressed as means ± SEM. $^*P < 0.05$ and $^{**}P < 0.01$ compared with the control group. $\#P < 0.05$ compared with the CD200 group.

groups (Cont. versus CD200: $P < 0.01$; CD47 versus CD200: $P < 0.05$), and the double group exhibited effects similar to those of the CD200 group. When human cytokine levels in the perfusates were analyzed, hCD200 suppressed the levels of TNF-α, IL-1β, and IL-6, and there was no difference in the suppressive activity between the hCD200 and double groups (Fig. 4D). The levels of C3a and C5a in the perfusates were also significantly lower in the CD200 group than in the control and hCD47 groups (Fig. 4E). Overall, these data showed that hCD200 overexpression in PECs effectively suppressed human cellular and antibody-mediated xenogeneic immune responses against the pTEVMP.

We also investigated the impact of hCD200 overexpression in PECs on thrombocoagulation responses in response to xenogeneic stimulation in an ex vivo pTEVMP circulation system. Scanning electron microscope analysis showed human platelet to pTEVMP lumen surfaces in each group (Fig. 5A). In the CD200 group, platelets rarely adhered to the surface of the pTEVMP lumen surface, whereas the pTEVMP in the control group showed high platelet adhesion (red triangles), and the CD47 and double groups showed partial platelet adhesion. As a result of immunofluorescence staining analysis with $CD41^+$ platelets and P-selectin ($CD62P^+$), which is released and expressed on the cell surface upon platelet activation (*28*), the CD200 group showed the lowest CD41 platelet and P-selectin expression (Fig. 5B). In particular, P-selectin in the CD200 group was significantly decreased compared with that in the CD47 and double groups ($P < 0.01$) (fig. S3). These data indicate that hCD200 in PECs suppressed the adhesion and infiltration of human platelets on pTEVMP tissues better than hCD47 and double overexpression. Similar results were also confirmed by flow cytometry of the perfusate, in which platelet-monocyte aggregate formation was suppressed by hCD200 (Fig. 5C). Furthermore, hCD200 in PECs suppressed both tissue factor (TF) expression in monocytes (Fig. 5C) and TF levels in the perfusates of the ex vivo circulation system (Fig. 5D). The exposure of TF to the circulation triggers the initiation and propagation of highly coordinated processes (*29*), and TF expression results from the activation of ECs in response to the deposition of xenoreactive antibodies and complement activation (*30*–*32*). Activated platelets may adhere to leukocytes and form circulating mixed aggregates, and their formation plays an important role in the initiation of thrombogenesis and inflammation (*33*). The levels of the thrombin-antithrombin complex

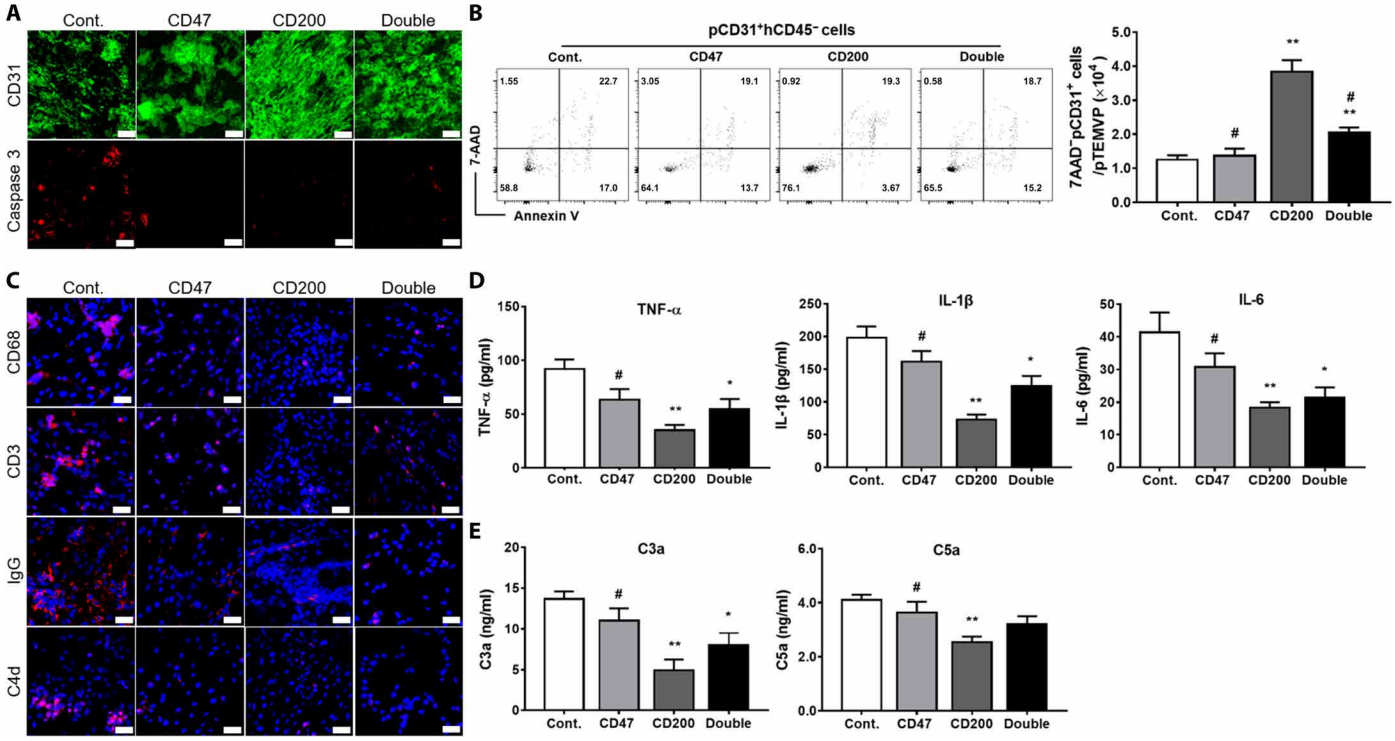

Fig. 4. hCD200 suppressed xenogeneic cytotoxicity and inflammation against the pTEVMP in the ex vivo circulation system of human whole blood. (**A**) Representative immunofluorescence images for human CD31 (green) and caspase 3 (red) in PECs in the pTEVMP lumen of each group. Magnification, ×200. Scale bars, 50 μm. (**B**) Flow cytometric analysis of the viability of PECs (annexin V/7-AAD) and absolute number of live PECs (7-AAD$^-$CD31$^+$) in pTEVMPs. (**C**) Representative immunofluorescence images for human CD68, CD3, IgG, C4d (red), and 4′,6-diamidino-2-phenylindole (DAPI) (blue) in the pTEVMP lumen of each group. Magnification, ×200. Scale bars, 50 μm. (**D**) Cytokine levels (TNF-α, IL-1β, and IL-6) in the perfusates. (**E**) Levels of C3a and C5a in the perfusates. $n = 4$ to 5 per group. Data are expressed as the means ± SEM. *$P < 0.05$ and **$P < 0.01$ compared with the control group. #$P < 0.05$ compared with the CD200 group.

(TAT), a marker for the activation of intravascular coagulation in the perfusates (*34*), were also suppressed by hCD200 (Fig. 5D). These results demonstrated that hCD200 overexpression in PECs effectively suppressed human thrombocoagulation responses by xenogeneic immune responses against the pTEMVP. Together, the ex vivo pTEVMP circulation system could provide an efficient xenogeneic immune response platform that enables dynamic and mechanistic characterization of both cellular and humoral xenogeneic immune responses.

Impact of anti-CD200 treatment on the xenogeneic immune response

To demonstrate the suppressive effect of hCD200 on the xenogeneic immune response more clearly, hCD200-overexpressing PECs were treated with anti-hCD200, and xenogeneic immune responses were evaluated by an ex vivo pTEVMP circulation system and in vitro assays. In xenogeneic coculture of PECs and hPBMCs, anti-hCD200 antibody abrogated the in vitro suppressive effects of hCD200 on phagocytosis (fig. S4A), apoptosis (annexin V$^+$pCD31$^+$) and cell death (7-AAD$^-$pCD31$^+$) (fig. S4B), and secretion of proinflammatory cytokines such as TNF-α, IL-1β, and IL-6 by PECs (fig. S4C).

In the ex vivo circulation system, while the CD200 group exhibited decreased apoptosis of PECs (caspase 3$^+$ cell density to pCD31$^+$ cells), hCD200 in PECs blocked with anti-hCD200 (CD200 + Anti-CD200 group) increased apoptosis of PECs up to the level in the control group (Fig. 6A and fig. S5A). However, in control PECs, there was no significant difference between anti-hCD200 treatment (control + Anti-CD200 group) and nontreatment (control group). The survival of PECs also showed a similar tendency to that of apoptosis. The number of 7-AAD$^-$pCD31$^+$ cells was significantly higher in the CD200 group, and the number in the CD200 + Anti-CD200 group was similar to those in the control group and control + Anti-CD200 group (Fig. 6B). Next, anti-hCD200 antibody treatment attenuated the beneficial effects of hCD200 on inflammatory cell infiltration as well as the deposition of IgG and C4d (Fig. 6C). In the CD200 + Anti-CD200 group, the CD68$^+$ macrophage and CD3$^+$ T cell densities as well as human C4d$^+$ and human IgG$^+$ area densities of the pTEVMP lumen increased by approximately 5.9, 5.5, 2.9, and 4.9 times compared with that of the CD200 group, respectively (fig. S5B). Moreover, we confirmed that anti-hCD200 antibody treatment abrogated the beneficial effects of hCD200 on inflammation, thrombocoagulation, and complement activation by xenogeneic immune responses. The beneficial effects of hCD200 overexpression in PECs on proinflammatory cytokine production were abrogated by anti-hCD200 treatment. The CD200 + Anti-CD200 group showed significantly higher levels of TNF-α, IL-1β, and IL-6 in the perfusate than the CD200 group ($P < 0.01$ for TNF-α; $P < 0.05$ for IL-1β and IL-6) (Fig. 6D). The levels of C3a, C5a, TF, and TAT, which were remarkably decreased in the CD200 group compared to the control group, showed no significant difference among the CD200 + Anti-CD200 group, control group, and control + Anti-CD200 group (Fig. 6, E and F).

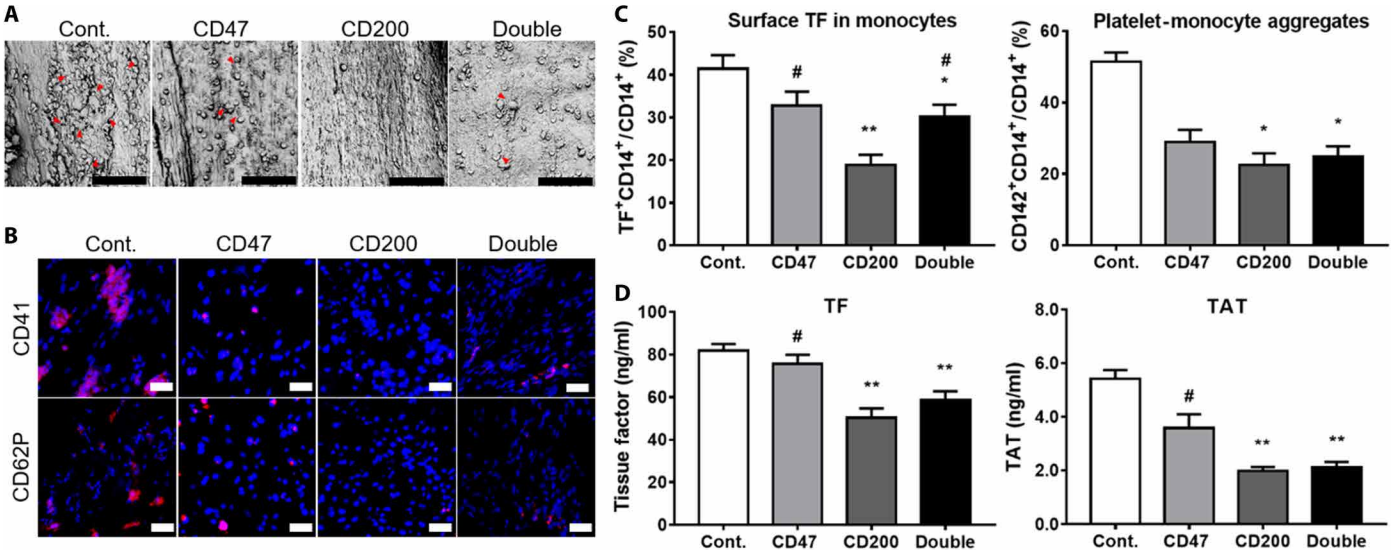

Fig. 5. hCD200 suppressed xenogeneic thrombocoagulation responses against pTEVMP in the ex vivo circulation system of human whole blood. (**A**) Scanning electron microscopic images of the pTEVMP lumens in each group. Red triangles indicate platelets. Scale bars, 50 μm. (**B**) Representative immunofluorescence images for human CD41, human CD62P (red), and DAPI (blue) in the lumen of pTEVMPs in each group. Scale bars, 50 μm. (**C**) Platelet-monocyte aggregate formation ($CD42b^+CD14^+$ cells) and monocyte surface-bound TF expression (TF^+CD14^+ cells) in the xenoperfusate were measured using flow cytometry. (**D**) Levels of TF and TAT in the perfusates. $n = 4$ to 5 per group. Data are expressed as the means ± SEM. $^*P < 0.05$ and $^{**}P < 0.01$ compared with the control group. $\#P < 0.05$ compared with the CD200 group.

Overall, these results support that suppressing xenogeneic immune responses in the CD200 group was mainly mediated by the overexpression of hCD200 in PECs.

Impact of hCD200 in PECs on pTEVMP xenograft survival in vivo

We confirmed the effect of hCD200 in PECs on the xenogeneic immune responses in vivo by xenografting pTEVMPs into humanized mice for 4 hours. Humanized mice were prepared by the transfer of hPBMCs and human plasma (Fig. 7A). Engraftment of human $CD45^+$ cells in the peripheral blood of humanized mice reached 58.2%, and the levels of human IgG and IgM 1 day after the transfer of human plasma were significantly higher in humanized mice than in nonobese diabetic–severe combined immunodeficient IL-2Rg null (NSG) mice without transfer (fig. S6, A and B). In the pTEVMP xenotransplantation to humanized mouse model, no vascular occlusion was noted at the anastomotic sites of the explanted xenografts (movie S1).

The in vivo xenogeneic immune response of hCD200 in PECs was similar to that of the ex vivo pTEVMP circulation system results. When thrombosis inside the vascular lumen of the pTEVMP xenografts was checked visually after explanting, thrombosis was prominent in the control group, whereas thrombosis was mild in the CD47, CD200, and double groups (Fig. 7B and fig. S7). Apoptosis of PECs (caspase 3^+ cell density to $pCD31^+$ cells) in the pTEVMP xenografts was decreased in the CD47, CD200, and double groups compared to the control group (Fig. 7C). In particular, the CD200 group showed a caspase 3^+ cell density that was 13.8 times lower than that of the CD47 group and 4.1 times lower than that of the double group, indicating that hCD200 in PECs has the greatest suppressive effect on apoptosis of PECs (fig. S8A). The viability of PECs in the pTEVMP xenografts (number of 7-AAD-$pCD31^+$ cells) was also significantly increased in the CD200 group compared to the control group ($P < 0.01$) and the CD47 group ($P < 0.05$) (Fig. 7D).

Next, hCD200 in PECs effectively suppressed the inflammatory cell infiltration and deposition of complement components in the pTEVMP xenografts. The $CD68^+$ macrophage and $CD3^+$ T cell densities and human $C4d^+$ and human IgG^+ area densities in the pTEVMP xenografts showed the lowest value in the CD200 group, followed by the double group, CD47 group, and control group (Fig. 8A and fig. S8B). When proinflammatory cytokine production was assessed using plasma collected from humanized mice xenografted with pTEVMPs, hCD200 in PECs of pTEVMP xenografts significantly suppressed plasma levels of TNF-α, IL-1β, and IL-6 (Fig. 8B). Furthermore, the CD200 group significantly suppressed the plasma levels of C3a and C5a (Fig. 8C) as well as those of TF and TAT (Fig. 8D) after xenotransplantation; however, there was no additive effect in the CD47 group and double group compared to the CD200 group. These results suggest that the pTEVMP could be used as a tool to assess the in vivo xenogeneic immune response of hCD200 via vascular xenotransplantation.

DISCUSSION

The present study demonstrates that the pTEVMP, which can mimic the microenvironment physiologically similar to native vessels in the human body, is successfully used to evaluate xenogeneic immune responses in vivo through a xenotransplantation model in humanized mice and ex vivo through a microfluidic system. Through this vascular platform, we demonstrated that overexpression of hCD200 in PECs can suppress human anti-pig xenogeneic immune responses and vascular xenograft rejection.

The TEVMP used in this study was fabricated simply through modified plastic compression using collagen-fibrin hybrid gels. Fibrin contained in hybrid gels is well known as an elastic polymer (*35*). For this reason, the vascular platform composed of hybrid gels had a higher tensile strain than the vascular platform composed of collagen. On the other hand, with regard to stiffness, the vascular

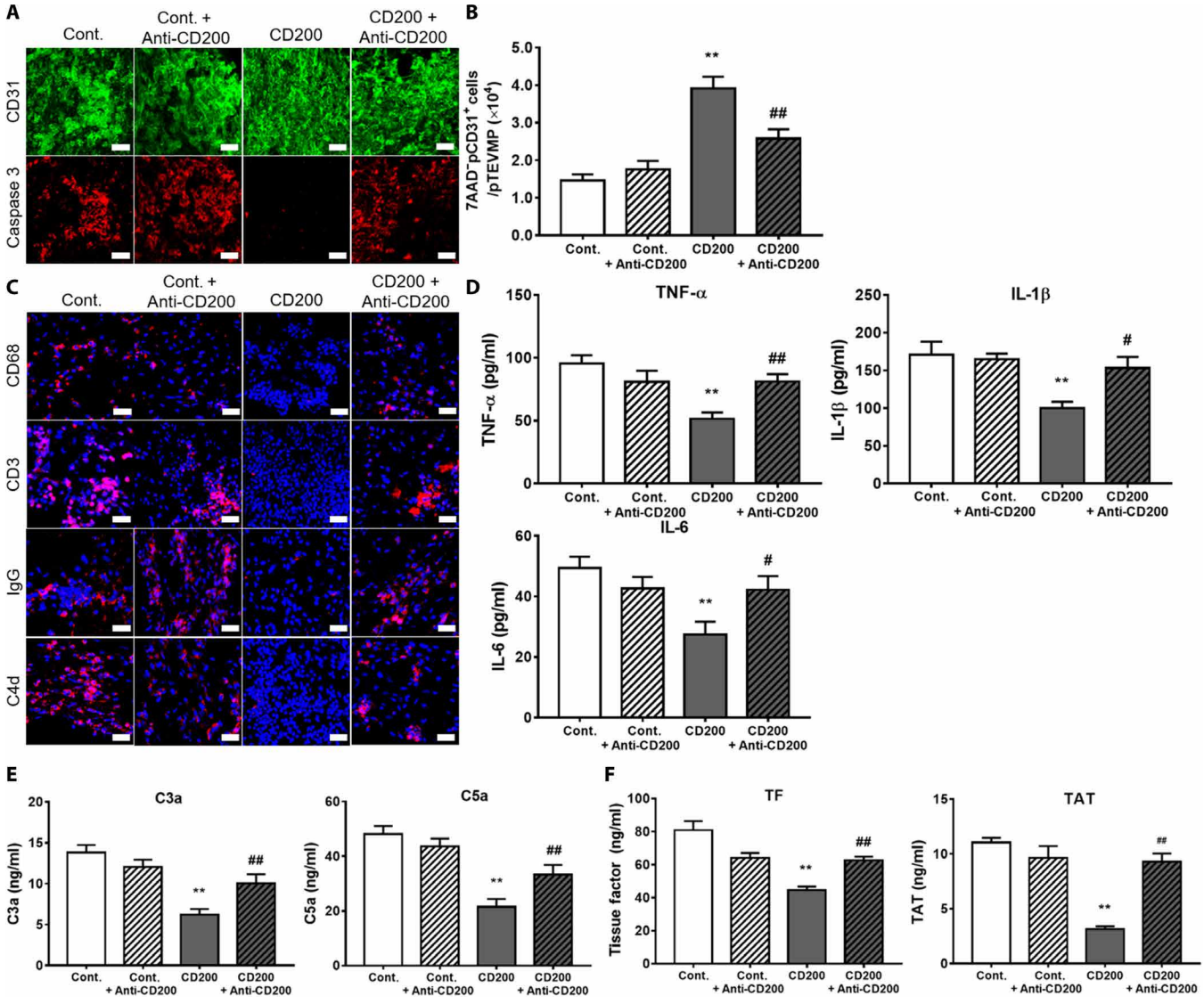

Fig. 6. Treatment with an inhibitory anti-CD200 antibody abrogated the beneficial effects of hCD200 in PECs on the xenogeneic immune responses against the pTEVMP in an ex vivo circulation system. (**A**) Representative immunofluorescence images for human CD31 (green) and caspase 3 (red) in PECs in the pTEVMP lumen of each group. Magnification, ×200. Scale bars, 50 μm. (**B**) Flow cytometric analysis of the absolute number of live PECs (7-AAD$^-$CD31$^+$) in pTEVMPs. (**C**) Representative immunofluorescence images for human CD68, CD3, IgG, C4d (red), and DAPI (blue) in the pTEVMP lumen of each group. Magnification, ×200. Scale bars, 50 μm. (**D**) Cytokine levels (TNF-α, IL-1β, and IL-6) in the perfusates. (**E**) Levels of C3a and C5a in the perfusates. (**F**) Levels of TF and TAT in the perfusates. $n = 4$ to 5 per group. Data are expressed as the means ± SEM. *$P < 0.05$ and **$P < 0.01$ compared with the control group. #$P < 0.05$ and ##$P < 0.01$ compared with the CD200 group.

platform composed of hybrid gels was lower than that composed of collagen gels. Collagen gels form bundles of thicker collagen fibers with fibrils, while fibrin gels form a fine network of wispy fibers (*36*). Since the hybrid gels are a mixture of collagen and fibrin, they are expected to show lower stiffness than the vascular platform composed of pure collagen. Plastic compression greatly increases the strength of hydrogels by excluding water from the hydrogels to form dense hydrogels (*10*). In addition, filamentous protein polymers, such as collagen and fibrin, are stiffened in response to compression, shear, or tension (*37*). When plastic compression was performed on the vascular platform composed of hybrid gels (TEVMP), the stiffness and elasticity were greatly increased, and the improvement of these mechanical properties increased the burst pressure of the TEVMP. Moreover, since the hybrid gels that compose the TEVMP are the ECM components of blood vessels, they provide a microenvironment similar to that of native vessels of PECs (*38*). Because of this, the adhesion of PECs was improved, and intercellular junction proteins were uniformly expressed, resulting in stable endothelialization on the lumen side of TEVMPs.

We applied the TEVMP, which has such good mechanical and physiological properties, as an ex vivo and in vivo platform in the study of the role of hCD200 in vascular xenograft rejection. As a porcine bioartificial artery, the pTEVMP endothelialized with PECs made it possible to investigate the impact of hCD200 overexpression on vascular xenogeneic rejection and cellular xenogeneic rejection, which were not possible in in vitro analysis via an ex vivo microfluidic

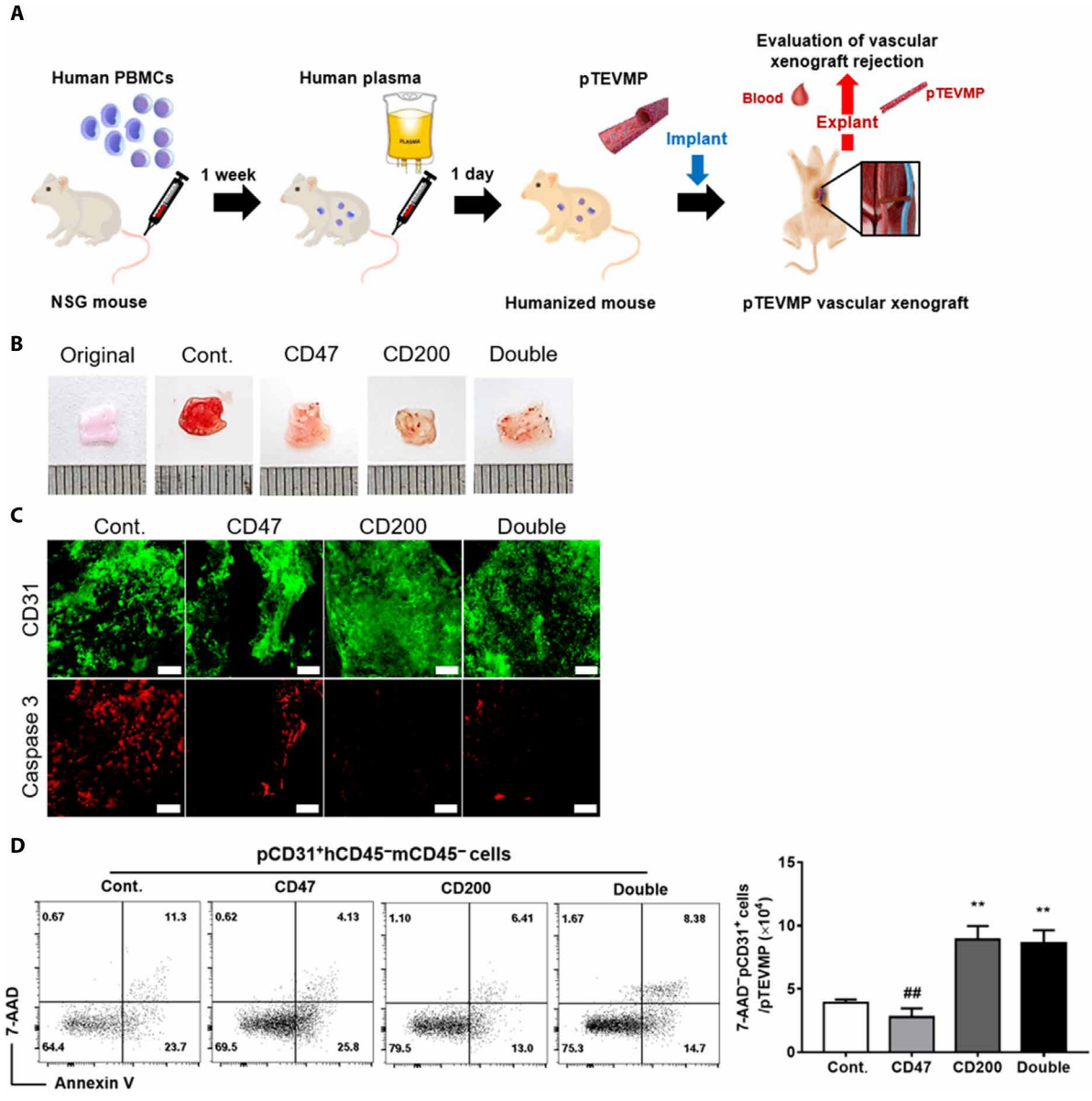

Fig. 7. hCD200 improved the survival of PECs in pTEVMP vascular xenografts in humanized mice. (**A**) Experimental scheme of pTEVMP xenotransplantation into humanized mice. (**B**) Gross findings of lumens of pTEVMP xenografts procured from humanized mice. "Original" indicates the pTEVMP before xenotransplantation. (**C**) Representative immunofluorescence images for human CD31 (green) and caspase 3 (red) in PECs in the lumen of pTEVMP xenografts. Magnification, ×200. Scale bars, 50 μm. (**D**) Flow cytometric analysis of the absolute number of live PECs (7-AAD$^-$CD31$^+$) in pTEVMP xenografts. $n = 5$ per group. Data are expressed as the means ± SEM. $^{**}P < 0.01$ compared with the control group. $^{\#\#}P < 0.01$ compared with the CD200 group.

system mimicking the human circulation system. These microfluidic systems to mimic physiological blood flow have been successfully used as screening tools before animal experiments (*39*, *40*). In the ex vivo microfluidic system, hCD200 overexpression suppressed apoptosis of PECs, infiltration of T cells and macrophages into pTEVMPs, and arterial deposition of IgG and C4d. Consistent with these findings, the concentrations of C3a and C5a as well as proinflammatory cytokines were decreased in the perfusate by overexpression of hCD200. In addition, hCD200 overexpression decreased the infiltration of platelets into pTEVMPs, platelet-monocyte aggregates, and the levels of TF and TAT in perfusates. These ex vivo assessment data more clearly demonstrated the effect of hCD200 on the xenogeneic immune response by showing that hCD200 overexpression suppressed xenogeneic antibody-mediated and thrombocoagulation responses toward vascular xenogeneic tissues as well as the xenogeneic cellular immune response, similar to in vitro analysis. Furthermore, treatment with anti-CD200 blocking antibodies abrogated the beneficial effects of hCD200 overexpression on the suppression of the xenogeneic immune response, suggesting that beneficial effects in the hCD200 overexpression group were mainly mediated by overexpression of hCD200 in PECs of the pTEVMP.

Genetically modified pig to nonhuman primate xenotransplantation models are the best preclinical xenotransplantation model, where acute vascular rejection and acute cellular rejection can occur.

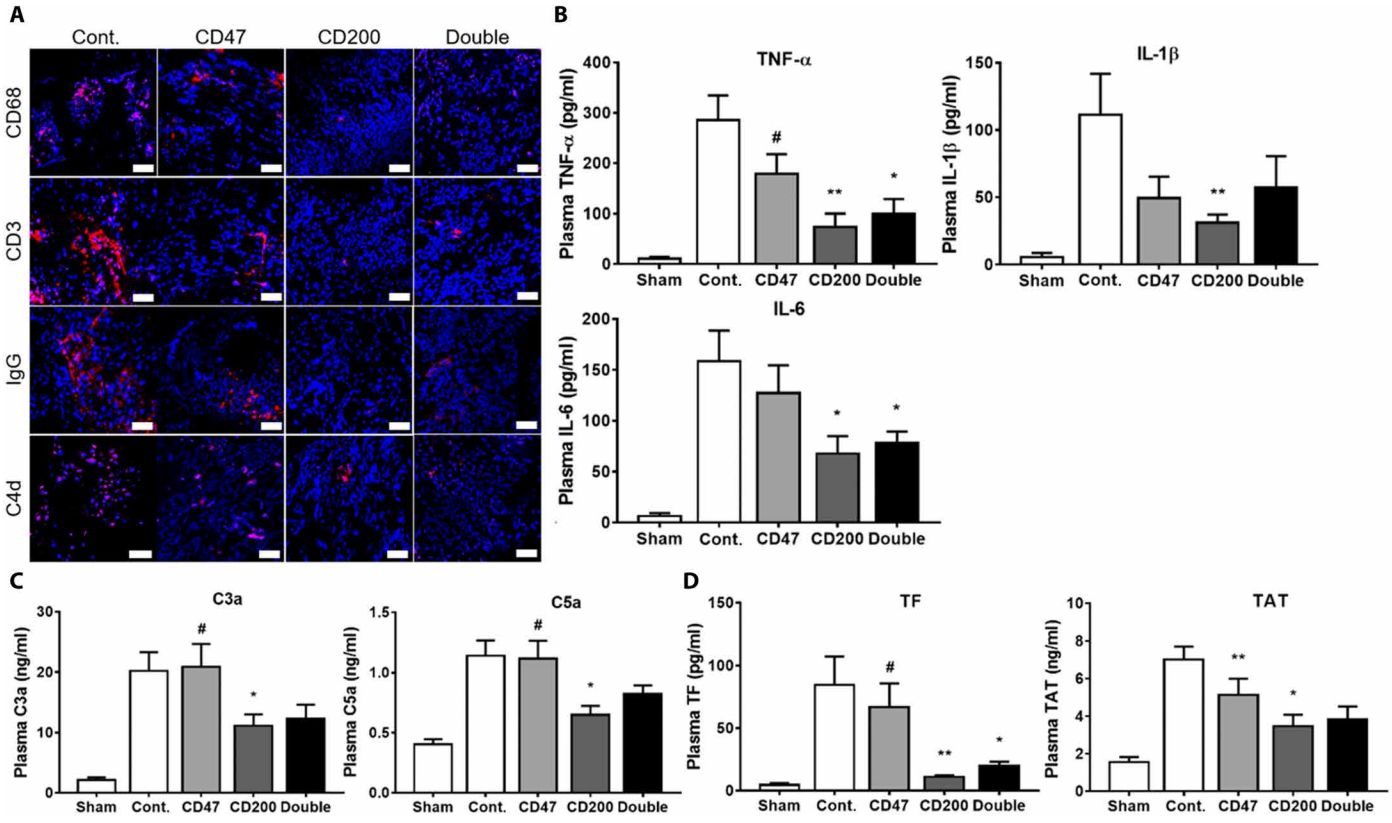

Fig. 8. hCD200 suppressed xenogeneic immune responses against pTEVMP vascular xenografts in humanized mice. (**A**) Representative immunofluorescence images for human CD68, CD3, IgG, C4d (red), and DAPI (blue) in the lumen of pTEVMP xenografts. Magnification, ×200. Scale bars, 50 μm. (**B**) Plasma cytokine levels (TNF-α, IL-1β, and IL-6) in humanized mice with pTEVMP xenografts. (**C**) Plasma levels of C3a and C5a in humanized mice with pTEVMP xenografts. (**D**) Plasma levels of TF and TAT in humanized mice with pTEVMP xenografts. $n = 3$ to 6 per group. Data are expressed as the means ± SEM. $^*P < 0.05$ and $^{**}P < 0.01$ compared with the control group. $\#P < 0.05$ compared with the CD200 group.

However, the high cost, rare source, and ethical dilemma of nonhuman primates led to low accessibility to research using this model, requiring a good screening animal model before final confirmation in nonhuman primate models. Recently, humanized mouse models have been successfully used for xenogeneic cell transplantation studies to study immune modulation strategies for acute cellular rejection (*41*, *42*). A previous study that used PEC transplantation into humanized mice showed that overexpression of hCD200 suppressed acute cellular xenograft rejection (*24*). However, this cellular xenotransplantation model cannot evaluate the impact of hCD200 overexpression on antibody-mediated xenogeneic immune responses and thrombocoagulation responses toward vascular xenografts beyond cellular xenografts. Since the developed pTEVMP can be fabricated to any desired size, we implanted the pTEVMP fabricated in a size that can be transplanted in humanized mice between the abdominal aorta and inferior vena cava to evaluate the effect of hCD200 overexpression on vascular xenograft rejection in vivo. hCD200 overexpression suppressed apoptosis of PECs, perigraft infiltration of T cells and macrophages, and graft deposition of IgG and C4d in humanized mice in parallel with the results of ex vivo perfusion experiments. Plasma levels of proinflammatory cytokines, complement activation, and coagulation activation in humanized mice were also suppressed by hCD200 overexpression in vascular xenografts. These data suggest that hCD200 overexpression in vascular xenografts suppresses vascular xenograft rejection, including xenogeneic antibody response, xenogeneic cellular response, and the activation of complement and coagulation systems.

CD200 has been shown to suppress phagocytic and cytotoxic activity as well as the secretion of proinflammatory cytokines by macrophages by binding to the CD200 receptor (*24*, *43*). Moreover, CD200 is reported to induce regulatory T cells and suppress antigen-presenting cells and T cells (*44*, *45*). In parallel, using pTEVMP, this study showed that CD200 overexpression suppressed the perigraft infiltration of macrophages and T cells as well as suppressed TNF-α, IL-1β, and IL-6. B cells also express the CD200 receptor, and CD200 can suppress antibody production after xenogeneic red blood cell sensitization (*45*, *46*). However, it is unlikely that overexpression of hCD200 directly suppressed B cells or antibody-mediated xenogeneic immune responses for a short time in this study. We speculate that the decreased deposition of IgG and C4d in vascular xenografts in the hCD200 overexpression group might have been indirectly derived from the suppression of T cells and innate immunity, such as macrophage activation, complement activation, and thrombocoagulation responses, against vascular xenografts.

Although hCD47 can suppress cellular xenograft rejection, such as hematopoietic cell, hepatocyte, and islet xenotransplantation, by suppressing macrophage activation by binding to CD172α, the beneficial effects of hCD47 overexpression in xenogeneic skin or heart transplantation were minimal, indicating that the roles of CD47 in xenografts are variable according to the cell types with hCD47

(*47*, *48*). The interaction between CD47 and thromboplastin, another receptor of CD47, might stimulate vascular xenograft rejection and diminish the protective effects of hCD47 on xenotransplantation (*49*). In the present study, we demonstrated more clearly through ex vivo and in vivo analysis using the TEVMP that the beneficial effects of hCD47 overexpression on vascular xenograft rejection were weaker than those of hCD200 overexpression. There were no additive effects between hCD200 overexpression and hCD47 overexpression on the suppression of xenogeneic immune responses against vascular xenografts, perhaps due to the overlapping actions of both molecules in macrophage suppression or the immune stimulatory effects of CD47 via thromboplastin.

Together, these data suggest that this study is very meaningful in two respects: (i) The TEVMP developed in this study can be applied to various vascular-related studies and used not only as an ex vivo platform by simulating in vivo a physiological environment similar to the circulatory system but also as an in vivo platform by implanting blood vessels into animals because of its high mechanical properties; and (ii) hCD200 has great potential for development into hCD200-transgenic pigs for organ xenotransplantation because of its superior suppressive effects on vascular xenograft rejection, beyond cellular xenograft rejection, compared with hCD47 that previous studies have established as an essential component of optimal genetically engineered pigs (*50*).

Furthermore, the next step in this study is to carry out research to overcome some limitations of the current platform. This vascular platform has a lower burst pressure than the arterial blood pressure of mice with higher blood pressure and faster heart rate compared to humans because of the absence of a tunica media layer composed of vascular smooth muscle cells in the arterial wall (*51*). Therefore, the pTEVMP was implanted between the abdominal aorta and inferior vena cava of humanized mice as an aortocaval shunt for in vivo evaluation. The aortocaval shunt developed high vascular flow and caused heart failure in the recipient. For this reason, long-term in vivo evaluation was not possible in this study. Aortic xenografts instead of aortocaval shunt xenografts could avoid this complication. To overcome these obstacles, future research plans include adding a tunica media layer using stromal cells to improve the mechanical strength of the vascular platform enough to withstand small animals' arterial blood pressure. The tunica media layer is a layer of smooth muscle (*52*). To mimic the smooth muscle layer in future research, we will need to add a layer including mesenchymal stem cells that can differentiate into smooth muscle cells in a hydrogel-based material with mechanical and physiological properties similar to those of the tunica media layer. Another limitation is that hPBMCs and plasma-based humanized mice are also not ideal for evaluating acute vascular xenograft rejection and chronic rejection because human hematopoiesis is not ongoing and there is a risk of graft-versus-host disease. Nevertheless, the pTEVMP has made it possible to simply and clearly investigate vascular xenograft rejection in vivo as well as ex vivo, and hPBMCs and plasma-based humanized mice are easy and convenient models as screening test for studying vascular xenograft rejection.

In summary, in this study, we developed the TEVMP, for application as an ex vivo and in vivo vascular platform to investigate the effect of hCD200 on the xenogeneic immune response. The TEVMP, fabricated by plastic compression using collagen-fibrin hybrid gels, which is an ECM component of blood vessels, can simply mimic native blood vessels due to its sufficient mechanical properties and stable 3D endothelialization. The TEVMP endothelialized with hCD200-overexpressing PECs could play a role similar to blood vessels of hCD200-transgenic pigs. pTEVMPs overexpressing hCD200 were introduced for ex vivo evaluation using a whole-blood microfluidic system and in vivo evaluation via xenotransplantation into humanized mice. In these evaluations, the survival of PECs, infiltration of human inflammatory cells, complement behavior, and thrombocoagulation responses were analyzed. It is noteworthy that in this evaluation using pTEVMP, it is possible to analyze vascular xenograft rejection, including thrombocoagulation responses that cannot be evaluated in 2D in vitro analysis or cellular xenotransplantation models. We clearly demonstrated ex vivo and in vivo that overexpression of hCD200 improves the survival of PECs and effectively suppresses the infiltration of human inflammatory cells, complement activation, and thrombocoagulation responses to a greater extent than overexpression of hCD47. On the basis of these results, we suggest that the TEVMP has a high potential as a platform to assess various vascular-related responses and that overexpression of hCD200 in donor pigs could be a promising strategy for suppressing vascular xenograft rejection.

MATERIALS AND METHODS

Preparation of the pTEVMP

A schematic of the TEVMP is presented in Fig. 1. TEVMPs were fabricated by modifying the plastic compression technique of collagen hydrogels to increase its mechanical properties, including elasticity (*53*). Rat tail collagen I (8.21 mg/ml; Corning) was diluted to 5 mg/ml using 10× phosphate-buffered saline (PBS; Gibco) and deionized water (DW), and the pH was raised to 7.0 using 1 N of sodium hydroxide (Sigma-Aldrich). To increase the elasticity, a hybrid solution mixed with fibrinogen solution (5 mg/ml in PBS; Sigma-Aldrich) and collagen solution in a 1:1 ratio was prepared. The hybrid solution was mixed with thrombin (50 U/ml; Sigma-Aldrich) at a volume ratio of 50:1 and then immediately transferred to a 1-ml syringe with a closed three-way Luer-Lock stopcock attached. A 21-gauge spinal needle stylet (diameter, 819 μm) was inserted in the center of the syringe and held in place with parafilm to create the TEVMP lumen. The hybrid solution loaded in the syringe was allowed to gel for 30 min at 37°C. After gelation of the hybrid solution, the hybrid gel with the inserted spinal needle stylet was taken out of the 1-ml syringe and laid onto a 0.8-μm membrane filter placed on 10 Kimwipes. The Kimwipes were folded in half, wrapped around the hybrid gel, and hung for approximately 2 min to remove water from the hybrid gel. Then, the hybrid gel was flipped so that the top side faced downward. The process was repeated to form TEVMPs with a uniform wall thickness of high-density gels. The TEVMPs were immersed in PEC media and allowed to stabilize in a 37°C incubator for 1 day.

To endothelialize TEVMPs with PECs, the fabricated TEVMPs were mounted in custom-made vascular perfusion chambers and sutured in place using 3-0 black silk sutures. After injecting PEC at a concentration of 1.5×10^7 cells/ml into the lumen of the TEVMP, the chamber was sealed and rotated at 37°C for 2 hours on a custom rotating platform at 10 rotations per hour to allow cell adhesion.

Characterization of the pTEVMP

To analyze the burst pressure, TEVMPs were loaded in perfusion chambers with one end plugged and the other attached to a differential pressure gauge. The burst pressure was measured by pressurizing

the TEVMP with PBS manually until rupture. The tensile properties of the TEVMP were measured by a universal testing machine (Instron 5966) at a 10-N load cell number and a crosshead speed of 10 mm/min ($n = 4$ per group). The tensile strength, elongation at break, and Young's modulus were obtained from the stress-strain curves. The cross-sectional surface morphologies of hydrogels were characterized by Scanning Electron Microscope (Inspect F, FEI, OR, USA) following Pt coating using a sputter coater.

Endothelialization in the pTEVMP lumen was analyzed using immunofluorescence staining. The TEVMPs endothelialized with PECs were fixed overnight in 4% paraformaldehyde (3 M) at 4°C and washed with PBS. The pTEVMPs were then permeabilized in 0.3% Triton X-100 (BIOSESANG) in PBS for 10 min and treated with blocking solution consisting of 4% bovine serum albumin (Sigma-Aldrich) dissolved in PBS for 1 hour. After that, anti-CD31 (1:25; Abcam) and anti–ZO-1 antibodies (1:50; Invitrogen) were added to confirm EC intercellular junctions and incubated at 4°C overnight. Thereafter, secondary antibody, Alexa Fluor 488 (1:500; Abcam), was added for 2 hours and washed with PBS. The samples were mounted using VECTASHIELD with 4′,6-diamidino-2-phenylindole (DAPI; Vector Labs). A LIVE/DEAD assay for PECs in the lumen of pTEVMPs was performed using calcein AM (1:2000; Invitrogen) and EthD-1 (1:500; Invitrogen) staining under static and perfused culture conditions for 1 day. Images were acquired using a laser scanning confocal microscope (Zeiss LSM700).

Preparation of PECs and human blood

Lentiviruses containing mock (pLenti6-CMV2-Flag), hCD200-expressing (pLenti6-Flag-CD200), or hCD47-expressing (pLenti6-Flag-CD47) vectors were produced by transient cotransfection with a three-plasmid system, as previously described (*24*). The control, hCD47-overexpressing, hCD200-overexpressing, and double (hCD200/hCD47)–overexpressing PEC lines were established by transduction of lentivirus containing each target molecule into PECs, as previously described (*24*). Human fresh whole blood was extracted from healthy volunteers, and hPBMCs were isolated from human whole blood using Ficoll-Hypaque (GE-Healthcare) density gradient separation. The study was approved by the Institutional Review Board (H-1411-020-623) of the Seoul National University Hospital.

In vitro phagocytosis, cytotoxicity, and cytokine assay

Transduced PECs and hPBMCs were stained with Violet CellTracker (Thermo Fisher Scientific) and carboxyfluorescein succinimidyl ester (CFSE; Thermo Fisher Scientific), respectively. Labeled PECs (2×10^5 per well) were incubated with labeled hPBMCs (4×10^5 per well) in 96-well plates. The proportion of CFSE/violet double-positive cells among the CFSE PBMCs was analyzed by flow cytometry to evaluate phagocytic function after 2 hours. After 6 hours, the cell mixtures were analyzed for viability by flow cytometric analysis after simultaneous staining with annexin V and 7-AAD (BD Biosciences, San Diego, CA). The levels of cytokine secretion were measured in the supernatant using an enzyme-linked immunosorbent assay (ELISA) kit after the coculture of PECs and hPBMCs for 48 hours. To inhibit hCD200, cocultured cells were incubated with inhibitory anti-CD200 antibody (5 mg/ml; BD Biosciences).

Ex vivo microfluidic system

The TEVMPs were endothelialized with control PECs with mock vector, hCD200-overexpressing PECs, hCD47-overexpressing PECs, and double (hCD47/hCD200)–overexpressing PECs. The microfluidic system consisted of custom-made vascular perfusion chambers, reservoirs, BioPharm Plus silicone tubing (Masterflex), and peristaltic pumps (Masterflex L/S 07522-30) that are used in various medical applications, including blood circulation (*49*). Fresh human whole blood was diluted twofold in Hank's balanced salt solution and perfused into pTEVMPs through a microfluidic system under physiological blood pressure conditions (1 ml/min of flow rate, 10 dyne/cm^2 of fluid shear stress, 37°C) for 4 hours. In another set of experiments, the pTEVMP circulatory system was pretreated with anti-CD200 antibody 1 hour before the perfusion of human whole blood.

Measurement of cytokines, complements, and coagulability

The levels of human cytokines such as TNF-α, IL-β, and IL-6 were measured by ELISA (BioLegend, San Diego, CA) according to the manufacturer's instructions. The levels of C5a and C3a were determined using ELISA (BD Biosciences). The levels of TF and TAT complexes were measured by ELISA (Abcam, Cambridge, UK).

Preparation of humanized mice

NSG mice were obtained from the Jackson laboratory (Bar Harbor, ME) and bred and maintained in a specific pathogen–free facility. The animal use protocols were approved by the Institutional Animal Care and Use Committee of Seoul National University (SNU-200306-5-1). The hPBMCs (2×10^7) were intravenously transferred to NSG mice, which received pooled human plasma (0.2 ml) a week after the transfer of hPBMCs (Fig. 7A).

pTEVMP xenotransplantation to humanized mice

After humanized mice were systemically heparinized (200 U/kg), pTEVMPs (with an internal diameter of 0.82 mm, 3 cm long) were implanted into the humanized mice as interpositional grafts between the abdominal aorta and inferior vena cava by side-to-side anastomosis using 10-0 Prolene. The pTEVMP xenografts were procured at 5 hours after transplantation.

Flow cytometric analysis

The pTEVMP tissues were cut into small fragments and then digested with frequent mixing for 20 min at 37°C in PBS containing fetal bovine serum (2%), EDTA (2.5 mM), collagenase type II (1 mg/ml; Sigma-Aldrich), and papain (10 mg/ml; Sigma-Aldrich). Cells were recovered from the digest by centrifugation and stained with 7-AAD (BD Bioscience) and the following antibodies: anti-pig CD31 (LCI-4, Bio-Rad, Hercules, CA), anti-human CD45 (HI30), anti-mouse CD45 (30-F11), and annexin V (BioLegend). Perfusates in the ex vivo pTEVMP circulation system were obtained after 5 hours of circulation and stained with the following antibodies: anti-human CD42b (HIPI, BioLegend), anti-human TF (NY2, BioLegend), and anti-human CD14 (61D3, Thermo Fisher Scientific). Each subset of cells was analyzed using an Attune NxT flow cytometer (Thermo Fisher Scientific) and FlowJo software (Tree Star, Ashland, OR).

Histological analysis

pTEVMPs were fixed in 4% paraformaldehyde for 24 hours at 4°C, embedded in an optimal cutting temperature compound (Leica), frozen using dry ice, and sectioned at a thickness of 30 μm by using a cryomicrotome (CM3050 S, Leica). Sections were dried on slides, fixed in 4% paraformaldehyde for 30 min at 37°C, stained with

hematoxylin and eosin using standard protocols, and observed under a light microscope (Olympus).

Immunofluorescence staining was performed to assess the viability of PECs, recruitment of human immune cells, and deposition of IgG and C4d. The following primary antibodies were used for staining: anti-pig CD31 (1:25; Abcam, Cambridge, UK), anti-human C4d (Millipore Sigma, St Louis, USA), anti–caspase 3 (1:50; 9H19 L2, Thermo Fisher Scientific), anti-human CD3 (1:50; OKT3, BioLegend), anti-human CD68 (1:100; Y1/82A, BioLegend), anti-human CD41 (1:25; HIP8, BioLegend), anti-human CD62P (1:100; AK4, BioLegend), and anti-human IgG (1:200; Bethyl Laboratories, Texas, USA). Next, secondary antibodies containing Alexa Fluor 488 or 594 (1:500; Abcam) and DAPI were added. Images were acquired on a Zeiss LSM700 laser scanning confocal microscope (Carl Zeiss AG, Oberkochen, Germany). The ImageJ plugin (https://imagej.nih.gov) was used for cell counting, and the positive cells were measured by counting four high-power fields (200×) per section. The positive area densities were calculated as the ratio of the $CD68^+$, $CD3^+$, $C41^+$, $CD62P^+$, IgG^+, and $C4d^+$ areas to the total cell area. The caspase 3^+ cell density was also calculated as the ratio of the caspase 3^+ area to the $CD31^+$ area.

Statistical analysis

All data are presented as the means ± standard error of the means (SEM) and were analyzed by analysis of variance (ANOVA) with post hoc comparisons. *P* values less than 0.05 were considered statistically significant. Statistical analyses were performed using GraphPad Prism 7 software (GraphPad Software, La Jolla, CA).

SUPPLEMENTARY MATERIALS

Supplementary material for this article is available at http://advances.sciencemag.org/cgi/content/full/7/22/eabg2237/DC1

View/request a protocol for this paper from *Bio-protocol*.

REFERENCES AND NOTES

1. S. Reardon, Organs-on-chips' go mainstream. *Nature* **523**, 266 (2015).
2. S. Kim, W. Kim, S. Lim, J. S. Jeon, Vasculature-on-a-chip for in vitro disease models. *Bioengineering* **4**, 8 (2017).
3. T. Osaki, T. Kakegawa, T. Kageyama, J. Enomoto, T. Nittami, J. Fukuda, Acceleration of vascular sprouting from fabricated perfusable vascular-like structures. *PLOS ONE* **10**, e0123735 (2015).
4. S. Han, Y. Shin, H. E. Jeong, J. S. Jeon, R. D. Kamm, D. Huh, L. L. Sohn, S. Chung, Constructive remodeling of a synthetic endothelial extracellular matrix. *Sci. Rep.* **5**, 18290 (2015).
5. H. Lee, W. Park, H. Ryu, N. L. Jeon, A microfluidic platform for quantitative analysis of cancer angiogenesis and intravasation. *Biomicrofluidics* **8**, 054102 (2014).
6. J. Ko, J. Ahn, S. Kim, Y. Lee, J. Lee, D. Park, N. L. Jeon, Tumor spheroid-on-a-chip: A standardized microfluidic culture platform for investigating tumor angiogenesis. *Lab Chip* **19**, 2822–2833 (2019).
7. S. Yasotharan, S. Pinto, J. G. Sled, S.-S. Bolz, A. Günther, Artery-on-a-chip platform for automated, multimodal assessment of cerebral blood vessel structure and function. *Lab Chip* **15**, 2660–2669 (2015).
8. L. E. Niklason, J. H. Lawson, Bioengineered human blood vessels. *Science* **370**, eaaw8682 (2020).
9. J. D. Drews, H. Miyachi, T. Shinoka, Tissue-engineered vascular grafts for congenital cardiac disease: Clinical experience and current status. *Trends Cardiovasc. Med.* **27**, 521–531 (2017).
10. M. Bitar, V. Salih, R. A. Brown, S. N. Nazhat, Effect of multiple unconfined compression on cellular dense collagen scaffolds for bone tissue engineering. *J. Mater. Sci. Mater. Med.* **18**, 237–244 (2007).
11. C. E. Ghezzi, N. Muja, B. Marelli, S. N. Nazhat, Real time responses of fibroblasts to plastically compressed fibrillar collagen hydrogels. *Biomaterials* **32**, 4761–4772 (2011).
12. M. G. Haugh, S. D. Thorpe, T. Vinardell, C. T. Buckley, D. J. Kelly, The application of plastic compression to modulate fibrin hydrogel mechanical properties. *J. Mech. Behav. Biomed. Mater.* **16**, 66–72 (2012).
13. O. V. Kim, R. I. Litvinov, J. Chen, D. Z. Chen, J. W. Weisel, M. S. Alber, Compression-induced structural and mechanical changes of fibrin-collagen composites. *Matrix Biol.* **60-61**, 141–156 (2017).
14. C. J. Phelps, C. Koike, T. D. Vaught, J. Boone, K. D. Wells, S.-H. Chen, S. Ball, S. M. Specht, I. A. Polejaeva, J. A. Monahan, P. M. Jobst, S. B. Sharma, A. E. Lamborn, A. S. Garst, M. Moore, A. J. Demetris, W. A. Rudert, R. Bottino, S. Bertera, M. Trucco, T. E. Starzl, Y. Dai, D. L. Ayares, Production of α1,3-galactosyltransferase-deficient pigs. *Science* **299**, 411–414 (2003).
15. L. Burdorf, A. Riner, E. Rybak, I. I. Salles, S. F. De Meyer, A. Shah, K. J. Quinn, D. Harris, T. Zhang, D. Parsell, F. Ali, E. Schwartz, E. Kang, X. Cheng, E. Sievert, Y. Zhao, G. Braileanu, C. J. Phelps, D. L. Ayares, H. Deckmyn, R. N. Pierson III, A. M. Azimzadeh, A. Dandro, K. Karavi, Platelet sequestration and activation during GalTKO.hCD46 pig lung perfusion by human blood is primarily mediated by GPIb, GPIIb/IIIa, and von Willebrand Factor. *Xenotransplantation* **23**, 222–236 (2016).
16. D. K. C. Cooper, A. Dorling, R. N. Pierson III, M. Rees, J. Seebach, M. Yazer, H. Ohdan, M. Awwad, D. Ayares, α1,3-galactosyltransferase gene-knockout pigs for xenotransplantation: Where do we go from here? *Transplantation* **84**, 1–7 (2007).
17. G. Chen, H. Qian, T. Starzl, H. Sun, B. Garcia, X. Wang, Y. Wise, Y. Liu, Y. Xiang, L. Copeman, W. Liu, A. Jevnikar, W. Wall, D. K. C. Cooper, N. Murase, Y. Dai, W. Wang, Y. Xiong, D. J. White, R. Zhong, Acute rejection is associated with antibodies to non-Gal antigens in baboons using Gal-knockout pig kidneys. *Nat. Med.* **11**, 1295–1298 (2005).
18. B. Ekser, P. Rigotti, B. Gridelli, D. K. C. Cooper, Xenotransplantation of solid organs in the pig-to-primate model. *Transpl. Immunol.* **21**, 87–92 (2009).
19. A. Lyons, A. M. Minogue, R. S. Jones, O. Fitzpatrick, J. Noonan, V. A. Campbell, M. A. Lynch, Analysis of the impact of CD200 on phagocytosis. *Mol. Neurobiol.* **54**, 5730–5739 (2017).
20. K. Minas, J. Liversidge, Is the CD200/CD200 receptor interaction more than just a myeloid cell inhibitory signal? *Crit. Rev. Immunol.* **26**, 213–230 (2006).
21. B. Sprangers, M. Waer, A. D. Billiau, Xenotransplantation: Where are we in 2008? *Kidney Int.* **74**, 14–21 (2008).
22. R. Gorczynski, J. Hu, Z. Chen, Y. Kai, J. Lei, A CD200FC immunoadhesin prolongs rat islet xenograft survival in mice1. *Transplantation* **73**, 1948–1953 (2002).
23. K. Yu, R. M. Gorczynski, Persistence of gene expression profile in CD200 transgenic skin allografts is associated with graft survival on retransplantation to normal recipients. *Transplantation* **94**, 36–42 (2012).
24. J.-J. Yan, T. Y. Koo, H.-S. Lee, W.-B. Lee, B. Kang, J.-G. Lee, J. Y. Jang, T. Fang, J.-H. Ryu, C. Ahn, S. J. Kim, J. Yang, Role of human CD200 overexpression in pig-to-human xenogeneic immune response compared with human CD47 overexpression. *Transplantation* **102**, 406–416 (2018).
25. J. L. Platt, The immunological hurdles to cardiac xenotransplantation. *J. Card. Surg.* **16**, 439–447 (2001).
26. G. Vidarsson, G. Dekkers, T. Rispens, IgG subclasses and allotypes: From structure to effector functions. *Front. Immunol.* **5**, 520 (2014).
27. K. Murata, W. M. Baldwin III, Mechanisms of complement activation, C4d deposition, and their contribution to the pathogenesis of antibody-mediated rejection. *Transplant. Rev.* **23**, 139–150 (2009).
28. B. Furie, B. C. Furie, The molecular basis of platelet and endothelial cell interaction with neutrophils and monocytes: Role of P-selectin and the P-selectin ligand, PSGL-1. *Thromb. Haemost.* **74**, 224–227 (1995).
29. B. A. Lwaleed, P. S. Bass, Tissue factor pathway inhibitor: Structure, biology and involvement in disease. *J. Pathol.* **208**, 327–339 (2006).
30. F. H. Bach, S. C. Robson, H. Winkler, C. Ferran, K. M. Stuhlmeier, C. J. Wrighton, W. W. Hancock, Barriers to xenotransplantation. *Nat. Med.* **1**, 869–873 (1995).
31. B. Gollackner, N. J. Mueller, S. Houser, I. Qawi, D. Soizic, C. Knosalla, L. Buhler, F. J. M. F. Dor, M. Awwad, D. H. Sachs, D. K. Cooper, S. C. Robson, J. A. Fishman, Porcine cytomegalovirus and coagulopathy in pig-to-primate xenotransplantation. *Transplantation* **75**, 1841–1847 (2003).
32. P. J. Cowan, S. C. Robson, A. J. F. d'Apice, Controlling coagulation dysregulation in xenotransplantation. *Curr. Opin. Organ Transplant.* **16**, 214–221 (2011).
33. C. Cerletti, C. Tamburrelli, B. Izzi, F. Gianfagna, G. de Gaetano, Platelet-leukocyte interactions in thrombosis. *Thromb. Res.* **129**, 263–266 (2012).
34. K. Deguchi, M. Noguchi, E. Yuwasaki, T. Endou, A. Deguchi, H. Wada, S. Murashima, M. Nishikawa, S. Shirakawa, K. Tanaka, M. Kusagawa, Dynamic fluctuations in blood of thrombin/antithrombin III complex (TAT). *Am. J. Hematol.* **38**, 86–89 (1991).
35. R. Tran, D. R. Myers, J. Ciciliano, E. L. Trybus Hardy, Y. Sakurai, B. Ahn, Y. Qiu, R. G. Mannino, M. E. Fay, W. A. Lam, Biomechanics of haemostasis and thrombosis in health and disease: From the macro- to molecular scale. *J. Cell. Mol. Med.* **17**, 579–596 (2013).
36. V. K. Lai, S. P. Lake, C. R. Frey, R. T. Tranquillo, V. H. Barocas, Mechanical behavior of collagen-fibrin co-gels reflects transition from series to parallel interactions with increasing collagen content. *J. Biomech. Eng.* **134**, 011004 (2012).
37. R. I. Litvinov, J. W. Weisel, Fibrin mechanical properties and their structural origins. *Matrix Biol.* **60**, 110–123 (2017).

38. J. Xu, G.-P. Shi, Vascular wall extracellular matrix proteins and vascular diseases. *Biochim. Biophys. Acta* **1842**, 2106–2119 (2014).
39. L. Burdorf, A. M. Azimzadeh, R. N. Pierson III, Xenogeneic lung transplantation models. *Methods Mol. Biol.* **2110**, 173–196 (2020).
40. A. Bengtsson, C. T. Svalander, J. Mölne, L. Rydberg, M. E. Breimer, Extracorporeal ("ex vivo") connection of pig kidneys to humans. III. Studies of plasma complement activation and complement deposition in the kidney tissue. *Xenotransplantation* **5**, 176–183 (1998).
41. M. Ji, X. Jin, P. Phillips, S. Yi, A humanized mouse model to study human immune response in xenotransplantation. *Hepatobiliary Pancreat. Dis. Int.* **11**, 494–498 (2012).
42. S. Yi, M. Ji, J. Wu, X. Ma, P. Phillips, W. J. Hawthorne, P. J. O'Connell, Adoptive transfer with in vitro expanded human regulatory T cells protects against porcine islet xenograft rejection via interleukin-10 in humanized mice. *Diabetes* **61**, 1180–1191 (2012).
43. M. C. Jenmalm, H. Cherwinski, E. P. Bowman, J. H. Phillips, J. D. Sedgwick, Regulation of myeloid cell function through the CD200 receptor. *J. Immunol.* **176**, 191–199 (2006).
44. R. Gorczynski, Z. Chen, I. Khatri, K. Yu, Long-term tolerance and skin allograft survival in CD200^{tg} mice after autologous marrow transplantation. *Transplantation* **98**, 1271–1278 (2014).
45. E. S. Rijkers, T. de Ruiter, A. Baridi, H. Veninga, R. M. Hoek, L. Meyaard, The inhibitory CD200R is differentially expressed on human and mouse T and B lymphocytes. *Mol. Immunol.* **45**, 1126–1135 (2008).
46. R. M. Gorczynski, M. S. Cattral, Z. Chen, J. Hu, J. Lei, W. P. Min, G. Yu, J. Ni, An immunoadhesin incorporating the molecule OX-2 is a potent immunosuppressant that prolongs allo- and xenograft survival. *J. Immunol.* **163**, 1654–1660 (1999).
47. H. Wang, Y.-G. Yang, Innate cellular immunity and xenotransplantation. *Curr. Opin. Organ Transplant.* **17**, 162–167 (2012).
48. K. Ide, H. Wang, H. Tahara, J. Liu, X. Wang, T. Asahara, M. Sykes, Y.-G. Yang, H. Ohdan, Role for CD47-SIRPα signaling in xenograft rejection by macrophages. *Proc. Natl. Acad. Sci. U.S.A.* **104**, 5062–5066 (2007).
49. M. Chen, Y. Wang, H. Wang, L. Sun, Y. Fu, Y.-G. Yang, Elimination of donor CD47 protects against vascularized allograft rejection in mice. *Xenotransplantation* **26**, e12459 (2019).
50. D. K. C. Cooper, H. Hara, H. Iwase, T. Yamamoto, Q. Li, M. Ezzelarab, E. Federzoni, A. Dandro, D. Ayares, Justification of specific genetic modifications in pigs for clinical organ xenotransplantation. *Xenotransplantation* **26**, e12516 (2019).
51. A. A. Mercadante, A. Raja, Anatomy, Arteries, in *StatPearls* (Treasure Island (FL), 2020).
52. A. M. Robertson, P. N. Watton, Mechanobiology of the arterial wall. *Trans. Biol. Media* **1**, 275–277 (2013).
53. J. C. Misra, S. Maiti, Peristaltic pumping of blood through small vessels of varying cross-section. *J. Appl. Mech.* **79**, 061003 (2012).

Acknowledgment

Funding: This research was financially supported by a grant of the Korea Health Technology R&D Project through the Korea Health Industry Development Institute (KHIDI), funded by the Ministry of Health and Welfare, Republic of Korea (grant number, HI20C0056) and National Research Foundation (NRF) of Korea, funded by the Ministry of Science and ICT (grant number, NRF-2021R1A2C2004634). **Author contributions:** Y.J. and J.Y. participated in the conception and design of the study. T.H.K. and J.-J.Y. performed most experiments. G.-M.L. and S.-K.L. prepared human and porcine cells. J.Y.J. performed animal studies. T.H.K., J.-J.Y., J.Y.J., B.S.K., J.J.C., S.H.K., Y.J., and J.Y. analyzed and interpreted the data. T.H.K. and J.-J.Y. wrote the original draft. T.H.K., J.-J.Y., J.Y.J., J.J.C., S.H.K., Y.J., and J.Y. wrote, reviewed, and edited the manuscript. **Competing interests:** The authors declare that they have no competing interests. **Data and materials availability:** All data needed to evaluate the conclusions in the paper are present in the paper and/or the Supplementary Materials. Additional data related to this paper may be requested from the authors.

Submitted 18 December 2020
Accepted 9 April 2021
Published 28 May 2021
10.1126/sciadv.abg2237

Citation: T. H. Kim, J.-J. Yan, J. Y. Jang, G.-M. Lee, S.-K. Lee, B. S. Kim, J. J. Chung, S. H. Kim, Y. Jung, J. Yang, Tissue-engineered vascular microphysiological platform to study immune modulation of xenograft rejection. *Sci. Adv.* **7**, eabg2237 (2021).